A Whole-Structure Approach to the Influence of Residual Stress on Fracture

12th International Conference on Fracture held on July 12-17, 2009 Ottawa, Ontario, Canada

C.J. Aird[1], D.J. Smith[1]
[1]*Solid Mechanics Group, Department of Mechanical Engineering, University of Bristol, Bristol, UK*

1 Introduction

It is known that the presence of tensile residual stress in a cracked structure can result in the load carrying capacity of the structure being much lower than that of an identical structure with no residual stress. Various researchers [1, 2, 3] have carried out tests to assess the influence of residual stress on the fracture of cracked components. Others [4, 5] have considered the problem of how to treat residual stresses in the fracture assessment of these components.

However, in engineering practice, a component is combined with other components to form a *structure*. This raises the possibility of long-range residual stresses being introduced in the structure as a result of misfits between components. In order to assess how the strength of a structure containing a cracked component is influenced by these long-range residual stresses, a whole-structure level approach (rather than a component-level approach) is required. The degree of change in load carrying capacity of such a structure depends not just on the initial level of long-range residual stress but also on how the residual stress changes as plastic deformation occurs in the structure prior to fracture.

This paper explores the influence of these long-range residual stresses on fracture from a whole-structure perspective. An idealised structure is described and results from whole-structure experiments, based on the idealised model, are presented. It is shown that the change in the load carrying capacity of the structure depends not only on the level of initial residual stress but also on the relative stiffness of the uncracked and cracked parts of the structure, as well as on the level of plastic crack mouth opening displacement (CMOD) prior to fracture.

2 Benchmark fracture tests

The work presented in this paper is based on fracture tests carried out on BS EN 10025 S355 J2G3 structural steel specimens [6] below the ductile to brittle transition temperature. Table 1 below gives the chemical composition of this steel, which

has a nominal minimum yield strength of 355MPa at room temperature.

Twenty compact tension C(T) fracture specimens were manufactured from a 75mm thick BS EN 10025 S355 J2G3 plate for the purpose of carrying out a set of initial benchmark fracture tests. These specimens were 25mm thick, with a 25mm crack length and a crack length to specimen width ratio of 0.50. The specimens were oriented such that the direction of crack growth corresponded to the short-transverse direction (the through thickness direction) and the loading direction corresponded to the long-transverse direction. In order to avoid the need for fatigue pre-cracking, the drawings specified that a 5mm long by 0.10mm wide notch was to be introduced in each specimen using a spark erosion process[1].

Ten of these C(T) specimens were tested at -125°C. Of this set of ten specimens, specimen S030 fractured at the lowest load while the highest fracture load corresponded to specimen S047. Crack mouth opening displacement was measured during these tests using a clip gauge, which was attached to knife edges mounted on the specimen. Force versus CMOD plots for each of these specimens are shown in Figure 1 a) and b).

The remaining ten specimens were tested at a lower temperature of -140°C. The force versus CMOD plots corresponding to the specimens with the lowest and the highest failure loads, specimens S034 and S027 respectively, are shown in Figure 1 c) and d).

3 The whole-structure approach

In order to determine how the load carrying ability of a cracked structure is influenced by the presence of long-range residual stress it is necessary to consider the response of the whole-structure as load is applied.

For example, consider the behaviour of an idealised structure consisting of two elements: a cracked element and an uncracked elastic element in parallel. Figure 2 a) shows the force versus displacement behaviour of such a structure for the case with no initial preload. The cracked element is labelled 'C(T)', and is an elastic-perfectly-plastic idealisation of specimen S047 shown in Figure 1 b). The uncracked elastic element is labelled 'Jig' and has a stiffness one half that of the cracked element. The load required to bring the structure to the point of fracture (point A) is 151kN. For the purpose of the following discussions, we define α as the ratio of the stiffness of the uncracked elastic element to the stiffness of the cracked element, so that in this case $\alpha = 0.5$.

[1]However, on inspection it was found that the notch widths were closer to 0.20mm than to 0.10mm.

Figure 2 b) shows the force versus displacement behaviour of the same structure with an initial preload of 25kN (rather than zero preload in Figure 2 a)). This initial preload is essentially an initial tensile long-range residual stress introduced into the cracked element, with balancing compressive residual stresses in the uncracked part. In this case the load required to bring the structure to the point of fracture (point A') is 113kN. Therefore, the presence of the initial 25kN preload has reduced the load carrying capacity of the structure to 0.75 times (113kN/151kN = 0.75) that of the structure with no preload.

However, this reduction in load carrying capacity is a function of the amount of plastic deformation prior to failure. To illustrate this, consider the case where the cracked element fails at the point at which plastic deformation begins (rather than after 0.70mm of plastic deformation). With no plastic deformation prior to failure, the failure load for the non-preloaded case is 97.5kN (point B), while the failure load for the preloaded case is 60kN (point B'). This gives a load carrying capacity of 0.62 times (60kN/97.5kN = 0.62) that of the non-preloaded structure.

Figure 3 shows how the load carrying capacity of the structure varies with the amount of plastic deformation prior to fracture. The y-axis label, 'Normalised force' refers to the force corresponding to the preloaded case divided by the force corresponding to the case with no initial preload. Values close to one therefore correspond to conditions where the difference between failure loads for the preloaded and non-preloaded cases are small. Conversely, values close to zero correspond to conditions where the initial preload (or long-range residual stress) has reduced the load carrying capacity of the structure a great deal. Points A" and B" correspond to the 0.75 and 0.62 values calculated above.

Figure 3 also shows that, for a given initial preload, the degree of change in the load carrying capacity of the structure depends on the relative stiffness of the two components. The line labelled $\alpha = 0$ corresponds to the extreme case where the uncracked elastic element has negligible stiffness compared with the cracked element. In this case, the load carrying capacity of the structure is independent of the amount of plastic deformation in the cracked element prior to fracture.

The line labelled $\alpha = \infty$ corresponds to the opposite extreme where the uncracked element has infinite stiffness compared with the cracked element. In this case, the load carrying capacity of the structure increases with increasing plastic deformation in the cracked element prior to fracture.

4 Whole-structure experiments

In order to explore the influence of residual stress on fracture from this whole-structure perspective experimentally, sixteen C(T) specimens were machined from

the steel plate used for the baseline tests described above, and a bespoke test jig was designed. Results from preliminary trials using this jig in conjunction with aluminium C(T) specimens at room temperature were presented in an earlier paper [7].

The jig was designed so that the relative stiffness of the specimen to the jig could be modified by using either stiff 250-maraging steel side-bars or less stiff Ti-6Al-4V side-bars in parallel with the C(T) specimen. The following procedure was used:

1. Insert either a pair of 250-maraging steel side-bars or a pair of Ti-6Al-4V side-bars.
2. Insert C(T) specimen.
3. Apply preload to assembly such that C(T) specimen carries tensile load and the side-bars carry a balancing compressive load.
4. Cool preloaded assembly to -125°C.
5. Increase applied load from 0kN up to load at which C(T) specimen fails by fast fracture. (Note that at this point the side-bars are still intact and only the cracked part of the structure has failed.)

Eight specimens were tested at -125°C using the jig in conjunction with the stiff 250-maraging steel side-bars. The remaining eight specimens were tested at -125°C using the jig in conjunction with the less stiff Ti-6Al-4V side-bars.

5 Results and discussion

Of the eight specimens tested in conjunction with the stiff 250-maraging steel side-bars, specimen S102 showed the least plastic deformation prior to fracture, and specimen S103 the most. The force versus CMOD results from these tests are shown in Figure 4 a) and b) respectively.

In the case of the eight tests carried out using the less stiff Ti-6Al-4V side-bars, the least plastic deformation was shown by specimen S115, and the most by specimen S118. The force versus CMOD results from these tests are shown in Figure 5 a) and b) respectively. Note that the gradient of the 'Jig' line is less steep than that of Figure 4, since the stiffness of the jig is determined by the stiffness of the side-bars used.

For the purpose of constructing normalised force plots (similar to that of Figure 3) for tests S103 and S118, the following calculations were made:

- First, the amount of plastic CMOD was estimated for each test by assuming that plastic deformation begins to accumulate in each specimen when the load reaches 40kN.

- Second, an equivalent linear jig stiffness was calculated for each test between the points A and B marked on Figures 4 b) and 5 b). (Figure 4 b) gives a jig stiffness for the test of specimen S103 of 244kN/mm. Figure 5 b) gives a stiffness of 127kN/mm for the test of specimen S118.)

Figure 6 shows the normalised force for test S103 calculated using the equivalent linear jig stiffness value of 244kN/mm mentioned above, versus the plastic component of CMOD. As in the case of the idealised model, upper and lower bound lines corresponding to $\alpha = \infty$ and $\alpha = 0$ extremes are also shown. The point labelled S103 corresponds to the failure of specimen S103. The point labelled S102 corresponds to the failure of specimen S102. Failure points for the remaining six specimens lie on the S103 line between these two points. Figure 7 shows the equivalent plot for test S118 using the corresponding linear jig stiffness of 127kN/mm.

Comparing these figures with Figure 3 (the equivalent plot for the idealised elastic-perfectly-plastic case described above) raises the following point. The $\alpha = 0$ line in Figure 3 is horizontal whereas the equivalent lines in Figures 6 and 7 are not. These lines have an initial positive gradient which decreases as a horizontal asymptote is approached with increasing plastic deformation. This difference stems from specimens S103 and S118 showing a smooth transition from elastic to increasingly perfectly-plastic like behaviour as opposed to the sudden discontinuous transition of the elastic-perfectly-plastic element.

Comparing Figures 6 and 7 with each other is also instructive. The main point to note is that the difference between the S103 line and the upper-bound line in Figure 6 is less than the difference between the S118 line and the upper-bound line in Figure 7. This stems from the different stiffness ratios associated with the two tests. The stiffness ratio α for test S103, which used the stiff 250-maraging steel side-bars, is 1.50. However, in the case of test S118, which used the less stiff Ti-6Al-4V side-bars, the stiffness ratio α is 0.87.

6 Concluding remarks

Both the idealised model and the results of the whole-structure tests have shown that when plastic CMOD precedes fracture, the reduction in load carrying capacity of the structure depends not only on the level of initial long-range residual stress but also on the stiffness ratio α, as well as the amount of plastic CMOD. This is because long-range residual stresses result from misfits between components. Any plastic CMOD which acts to reduce the misfit will therefore have the effect of reducing the residual stress. By how much the residual stress reduces for a given amount of plastic CMOD depends in turn on the stiffness ratio.

However, when linear elastic conditions apply, such that no plastic CMOD precedes fracture, the reduction in load carrying capacity of the structure depends only on the

level of initial residual stress.

Finally, from the point of view of structural integrity assessments, the main implication of the work presented in this paper is that, where long-range residual stresses exist in a structure and plastic CMOD precedes failure, it is not enough to know the fracture properties of a cracked component in isolation. Knowledge of the whole-structure is required, since the boundary conditions associated with the component are governed by the surrounding structure.

References

[1] X. R. Wu, The effect of welding residual stress on brittle fracture of plates with surface cracks, Engineering Fracture Mechanics 19 (1984) 427–439

[2] Y. Ueda, Y. C. Kim, K. Kajimoto, M. Fujii, Y. Hagiwara, H. Takashima, Brittle fracture strength of repair weldments in thick plate, Naval Architecture and Ocean Engineering 24 (1986) 169–184

[3] J. K. Sharples, D. J. Sanderson, B. R. Bowdler, A. Wightman, R. Ainsworth, Experimental programme to assess the effect of residual stresses on fracture behaviour, in: American Society of Mechanical Engineers Pressure Vessels and Piping Conference, Honolulu, USA, 1995, volume 304, pp. 539–551

[4] R. A. Ainsworth, The treatment of thermal and residual stresses in fracture assessments, Engineering Fracture Mechanics 24 (1) (1986) 65–76

[5] D. Green, J. Knowles, The treatment of residual stress in fracture assessment of pressure vessels, in: American Society of Mechanical Engineers Pressure Vessels and Piping Conference, New Orleans, USA, 1992, volume 233, pp. 237–247

[6] BS EN 10025. Hot rolled products of non-alloy structural steels. Technical delivery conditions., BSI British Standards (1993)

[7] C. J. Aird, S. Hadidi-Moud, C. E. Truman, D. J. Smith, Impact of residual stress and elastic follow-up on fracture, Journal of ASTM International 5 (8) (2008)

C	Si	Mn	P	S
0.22	0.55	1.60	0.035	0.035

Table 1: Chemical composition (by % weight) of BS EN 10025 S355 J2G3 steel

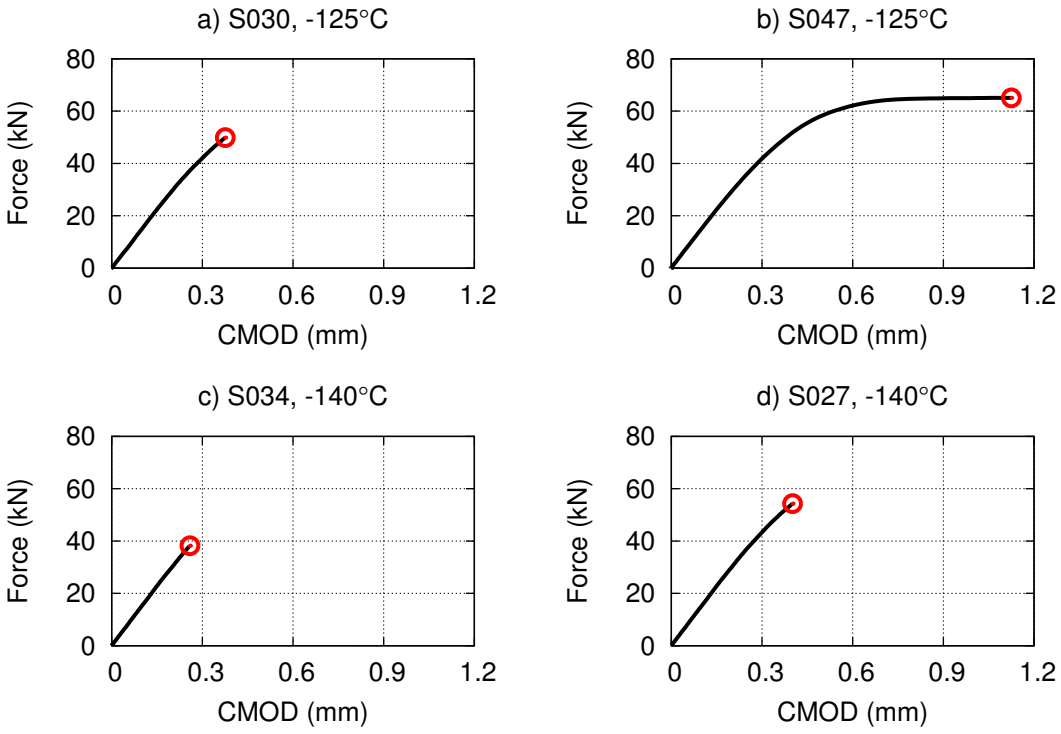

Figure 1: Force versus crack mouth opening displacement for 25mm thick BS EN 10025 S355 J2G3 steel C(T) specimens at -125°C and -140°C

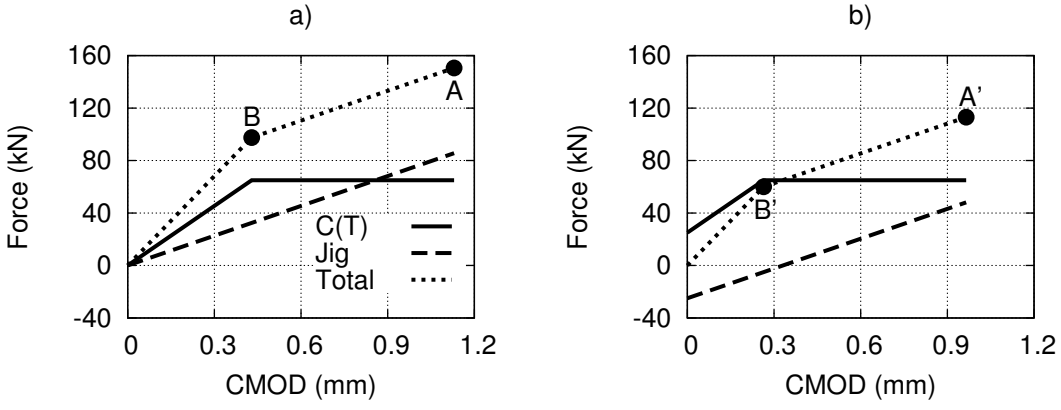

Figure 2: Force versus crack mouth opening displacement for structure a) without and b) with preload

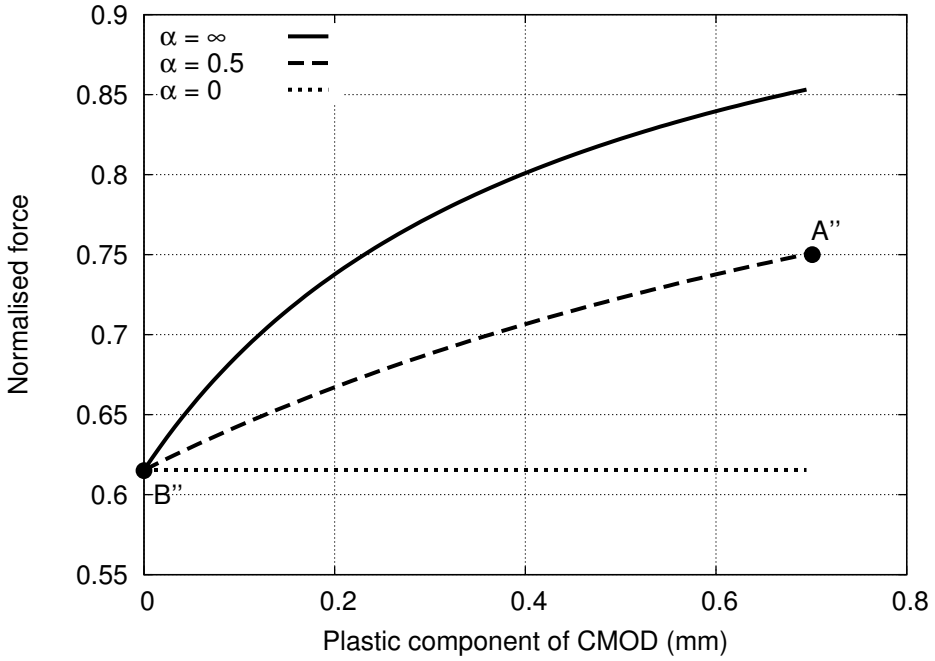

Figure 3: Normalised force versus plastic component of crack mouth opening displacement for structure of Figure 2

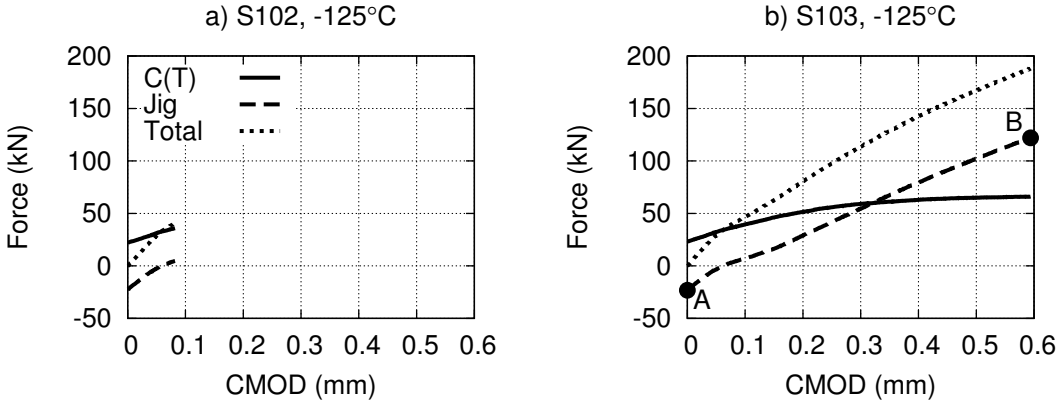

Figure 4: Force versus crack mouth opening displacement for a) specimen S102 and b) specimen S103 in jig with 250-maraging steel side bars at -125°C

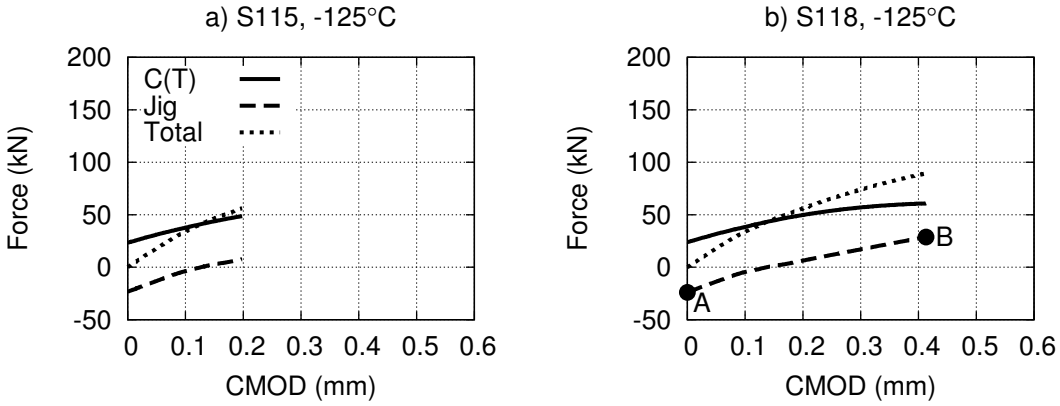

Figure 5: Force versus crack mouth opening displacement for a) specimen S115 and b) specimen S118 in jig with Ti-6Al-4V side bars at -125°C

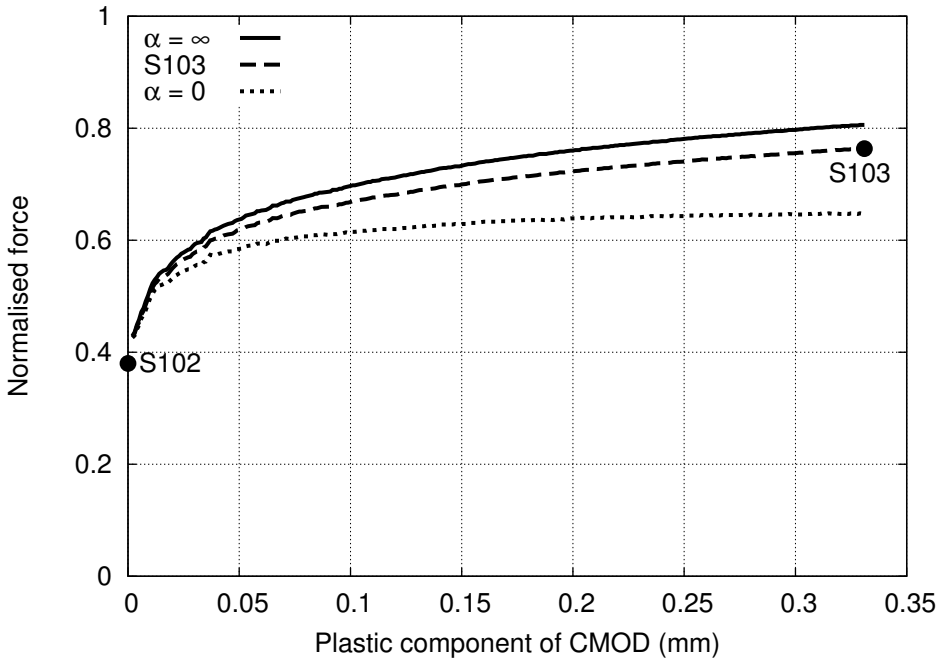

Figure 6: Normalised force versus plastic component of crack mouth opening displacement for specimen S103 in jig with 250-maraging steel side bars at -125°C

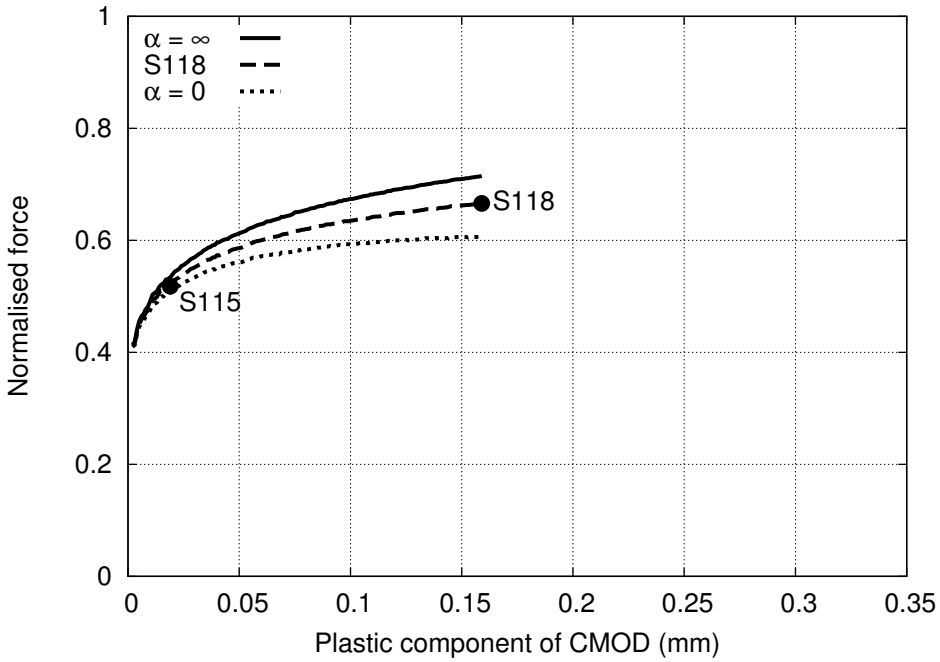

Figure 7: Normalised force versus plastic component of crack mouth opening displacement for specimen S118 in jig with Ti-6Al-4V side bars at -125°C